



Article

Comprehensive Evaluation of Wet-Spun Polyhydroxyalkanoate Fibres: Morphology, Crystallinity, and Thermal Properties

Marta A. Teixeira *, Inês Leite, Raquel Gonçalves, Helena Vilaça , Catarina Guise and Carla Silva 

CITEVE—Technological Centre for Textile and Clothing of Portugal, 4760-034 Vila Nova de Famalicão, Portugal; ileite@citeve.pt (I.L.); rgoncalves@citeve.pt (R.G.); hvilaca@citeve.pt (H.V.); cguise@citeve.pt (C.G.); cjsilva@citeve.pt (C.S.)

* Correspondence: mteixeira@citeve.pt

Highlights

What are the main findings?

- Wet-spun fibres were successfully produced from modified P(3HB) variants, demonstrating their suitability for fibre formation;
- Blended fibres exhibited smaller, more uniform diameters compared to fibres made from individual (neat) polymers

What is the implication of the main finding?

- The successful wet-spinning of modified P(3HB) variants confirms their suitability for fibre production, supporting their potential as sustainable alternatives to conventional plastic-based fibres;
- The enhanced uniformity and reduced diameter of blended fibres indicate that polymer blending is an effective strategy to improve the processability and structural quality of PHA-based fibres, broadening their application potential.

Abstract

In response to increasing environmental concerns, significant efforts have been made to reduce our reliance on fossil fuel-based plastics, driving the development of sustainable alternatives such as polyhydroxyalkanoates (PHAs). This study investigates the processing of various PHAs into fibres, focusing on their morphological, thermal, and mechanical properties. Different PHAs were spun into fibres at a 15% (*w/v*) concentration using wet-spinning techniques. Among the PHAs studied, commercially available PHBHHx, used as a reference, exhibited spongy morphology in the fibres and demonstrated thermal vulnerability due to its rapid degradation. Blended fibres showed enhanced morphological and mechanical properties compared with neat fibres. In Fourier-transform infrared spectroscopy (FTIR), no differences were observed between the unprocessed polymers and the wet-spun polymeric fibres, indicating that the wet-spinning process did not affect the molecular structure of the polymers. Thermal and mechanical evaluations confirmed the miscibility between the polymers in the blends. Overall, these results highlight, for the first time, the successful production of wet-spun fibres from two modified P(3HB) variants, individually, in combination with each other, and in blends with the well-established commercial PHA, PHBHHx. However, this study also underscores the need to optimise feed rates to enhance fibre production efficiency and mechanical strength, thereby broadening their potential for various applications.



Academic Editor: Martin J. D. Clift

Received: 26 June 2025

Revised: 31 July 2025

Accepted: 12 August 2025

Published: 21 August 2025

Citation: Teixeira, M.A.; Leite, I.; Gonçalves, R.; Vilaça, H.; Guise, C.; Silva, C. Comprehensive Evaluation of Wet-Spun Polyhydroxyalkanoate Fibres: Morphology, Crystallinity, and Thermal Properties. *Fibers* **2025**, *13*, 111. <https://doi.org/10.3390/fib13080111>

Copyright: © 2025 by the authors. Licensee MDPI, Basel, Switzerland. This article is an open access article distributed under the terms and conditions of the Creative Commons Attribution (CC BY) license (<https://creativecommons.org/licenses/by/4.0/>).

Keywords: polyhydroxyalkanoates; biodegradable polymers; wet spinning; fibre morphology; thermal properties; mechanical properties; sustainability

1. Introduction

Owing to the excellent properties of plastics, such as high versatility, high strength-to-weight ratio, low weight, resistance to physical and chemical degradation, and low cost, they can be found in various sectors [1]. Packaging, construction, textiles, electronics, transportation, food, healthcare, and energy are just some examples of the industries widely using plastics [2]. However, increased environmental awareness has led to the reduction and replacement of fossil fuel plastics, which has consequently contributed to the development of bioplastics [3]. It is estimated that the global bioplastic market size will grow at 24.2% until 2029, when it will reach USD 45.2 billion (from USD 27.84 billion in 2025). Regarding the bioplastic European market, it is expected to expand at a compound annual growth rate of 18.3% up to 2030 [4]. Bioplastics can be defined as plastics that (i) are made from renewable resources ('bio-based'), (ii) are biodegradable, (iii) are made through biological processes, or (iv) a combination of these [5]. These bioplastics have various benefits over petroleum-based plastics, including a lower carbon footprint, energetic efficiency, and biodegradability, and might have improved material properties. Nonetheless, bioplastics often exhibit poorer properties such as thermal instability, low melt strength, and poor processability that can limit their application [6]. In addition, their cost, production scale, recyclability, and legislation are some current challenges that bioplastics still face [7]. The most widely used bioplastics on the global market include non-biodegradable polymers such as polyethylene (bio-PE), polyethylene terephthalate (bio-PET), and polypropylene (bio-PP). Biodegradable alternatives include polybutylene succinate (PBS), polybutylene adipate terephthalate (PBAT), polylactic acid (PLA), thermoplastic starch, and polyhydroxyalkanoates (PHAs) [8,9]. Among these bioplastics, polymers from the PHAs group have attracted significant attention as alternatives to petroleum-based plastics [10]. PHAs are a class of biodegradable polyesters that can be produced biotechnologically by a wide range of microorganisms as intracellular carbon and energy storage materials or synthesised chemically via polymerisation. These biopolymers are typically derived from renewable feedstocks such as biomass, organic waste, and fatty acids [11]. More than 150 different PHA monomers have been identified, contributing to a diverse class of materials with tuneable mechanical properties and degradation rates [12,13]. PHAs exhibit substantial variations in chain length and composition, and their molecular weights typically range from 50,000 to 1,000,000 Da [14]. Based on their monomer structures, PHAs are classified into short-chain-length (scl), medium-chain-length (mcl), and long-chain-length (lcl) types. scl-PHAs are composed of hydroxy fatty acids with carbon chain lengths ranging from C3 to C5, whereas mcl-PHAs contain C6 to C14 monomers, and lcl-PHAs consist of hydroxy fatty acids with chains longer than C14 [15]. Among them, poly(3-hydroxybutyrate) (P3HB), a scl-PHA, is the most extensively studied due to its microbial origin and biodegradable nature [16–18]. However, its industrial application is limited by its high crystallinity, brittleness, and thermal degradation, which occurs just above its melting temperature. These unfavourable properties are attributed to its isotactic structure, resulting from its biosynthetic production pathway [19]. To address these limitations, approaches such as the incorporation of comonomers by using chain extension reactions to create tailored block copolymers with hard and soft segments or blending with other biopolymers have been the most employed techniques to disrupt the crystalline structure of isotactic P3HB [20]. Among these approaches, blending stands out

for its practicality and suitability for industrial-scale implementation [19]. These strategies reduce crystallinity by introducing structural irregularities, which in turn enhance the material's thermal and mechanical behaviour. One effective approach involves the use of chemically synthesised atactic P(3HB), an amorphous variant that can be blended with the isotactic form to tailor the polymer's properties for enhanced performance [21]. This atactic variant is typically obtained through the ring-opening polymerisation (ROP) of racemic β -butyrolactone, which is the most reported method. Alternative synthetic routes, including conventional polycondensation and, more recently, self-polycondensation of hydroxy acids or their esters, have also been explored [22]. In this study, blends of P3HB with chemically synthesised PHAs such as a-P3HB were used. The specific samples used were designated PHA.C.3.3.1.4 and PHA.A.2.3.1.1.

In addition to these structural changes to PHAs, the investigation of new processing techniques is important for further expanding the potential application of these biopolymers [7].

The processing of PHAs into fibres can be a beneficial strategy to create and design more suitable applications and to add specific functional properties [23]. Wet spinning is an industrialised fibre production technique, which involves the injection of a polymeric solution into a coagulation bath composed of a non-solvent or a poor solvent of that polymer. It results in fast precipitation of the polymer, as well as solvent removal, and coagulant penetration, forming solid microfibers [24,25]. This technique, comparatively to melt spinning, allows for low processing temperatures, being a preferable method for the processing of PHAs to avoid their thermal degradation [26]. The production of wet-spun PHA fibres, such as P3HB [27], poly-4-hydroxybutyrate (P4HB) [28], PHBV [29,30], PHBHHx [31], and poly(3-hydroxybutyrate-co-4-hydroxybutyrate) (P3HB4HB) [32], has already been reported in the literature. However, research on wet-spun fibres composed of chemically synthesised PHA, which exhibit enhanced elongation and tuneable crystallinity compared with neat P3HB, represents a highly exploratory pathway.

To date, only a few studies have explored such systems; for instance, Algoz [33] incorporated PLA, whereas Pecorini [34] introduced hydroxyapatite into PHA matrices. This scarcity of work may be attributed to several technical challenges, including solvent compatibility, phase miscibility (i.e., dispersion uniformity), coagulation kinetics, and the complexity of post-spinning treatments such as fibre drawing and mechanical stabilisation [35]. Therefore, the exploration of blends involving different types of PHAs holds considerable promise for enhancing fibre performance. It is well established that wet-spun fibres often exhibit high porosity, variable cross-sectional dimensions, diverse internal morphologies, and a wide range of physical and chemical properties [36,37].

To the best of the authors' knowledge, this study represents the first investigation into the development of wet-spun fibres from two partially synthesised P(3HB) variants—PHA.C.3.3.1.4 and PHA.A.2.3.1.1—produced via a novel self-polycondensation method using racemic ethyl 3-hydroxybutyrate. In addition to examining these materials individually, their blends with each other and with PHBHHx were also explored.

The primary aim was to establish optimal conditions for polymer dissolution and coagulation within the wet-spinning process. Furthermore, to evaluate the impact of polymers structures on fibre formation and resulting material properties, an in-depth physicochemical characterisation was performed on neat and blended fibres. This work advances the understanding of PHA-based fibre systems, offering new perspectives for the design of bio-derived materials.

2. Materials and Methods

2.1. Materials and Reagents

PHBHHx powder was purchased from Bluepha (Beijing, China) and partially synthesised P3HBs (PHA.C.3.3.1.4 and PHA.A.2.3.1.1) in a granular form were kindly provided by the University of Kaiserslautern (Kaiserslautern, Germany). These are blends of isotactic P3HB with chemically synthesised PHAs, such as the α -P3HB synthesised by self-condensation, as reported by Almustafa et al. [21]. The blending of P3HB with chemically synthesised PHAs aims to facilitate their processing via wet spinning. The average molecular weight (Mw) and the polydispersity (PD) expressed by the ratio of Mw/Mn (where Mn means the average molecular weight) of each polymer are shown on Table 1. Glacial acetic acid, chloroform, and ethanol were obtained from Fisher Scientific™ (Porto Salvo, Portugal), while calcium chloride was purchased from Carlo Erba Reagents (Lisbon, Portugal). Plastic luer lock syringes of 5 mL and with 21G needles with bevelled tips with dimensions of 0.80×40 mm were acquired from VWR (Carnaxide, Portugal). All reagents were used without further purification.

Table 1. Characteristics of raw materials.

Polymer	Mw (Da)	Mw/Mn
PHBHHx	291,000	4.51
PHA.A.2.3.1.1	256,423	3.30
PHA.C.3.3.1.4	215,659	2.10

2.2. Study on Processing Parameters of the Wet-Spinning Technique

Concentrations of 10%, 15%, and 20% (w/v) were selected to evaluate the solubility of each PHA in pure chloroform. The boiling point of chloroform (61.2°C) was considered to prevent solvent evaporation during the dissolution process [38,39]. A range of polymer blend ratios was investigated, encompassing pure individual PHAs (100/0) and blends at 90/10, 80/20, 70/30, 60/40, and 50/50 (w/w) proportions across all PHA combinations studied. PHBHHx powder and PHA granules were combined with pure chloroform and heated to its boiling point in a covered beaker under constant stirring. The mixtures were maintained at $\approx 60^\circ\text{C}$ until the complete dissolution of each respective PHA was achieved.

To identify the optimal coagulation bath conditions, drop tests were conducted in various baths. The coagulation baths tested included distilled water (at temperatures ranging from cold to hot), ethanol, acetone, propanol, methanol, sodium hydroxide, ethyl acetate, and hexanol. Apart from distilled water, all these non-solvents were tested at room temperature (RT) due to their high volatility. During the drop tests, polymer solutions were added dropwise to the potential coagulation baths in glass vials, and tweezers were used to stretch the polymer drops during coagulation.

2.3. Production of Wet-Spun PHA Fibres

Polymeric solutions of the different PHAs were dissolved at 15% (w/v) in pure chloroform. These solutions were continuously stirred at RT for 2 h. Each polymer was first wet-spun individually to produce neat fibres and subsequently processed as blends consisting of 70/30% (v/v) mixtures of PHA.C.3.3.1.4/PHBHHx and PHA.C.3.3.1.4/PHA.A.2.3.1.1, respectively. These blends were also prepared as 15% (w/v) solutions in pure chloroform. The aim of the blending process was to combine the distinct properties of each polymer (for example, crystallinity) to achieve enhanced final characteristics in the resulting fibres.

All PHA solutions were extruded at a feed rate of 0.07 mL/min, which was identified as the optimal rate to ensure stable and continuous extrusion into the ethanolic coagulation bath at RT. The spun fibres, formed immediately upon immersion of the PHA solutions

into the pure ethanolic coagulation bath, were manually pulled slowly using tweezers and wound onto a yarn cone. Subsequently, the fibres were dried for 24 h at RT and washed for 5 min to remove residual non-solvent and solvent from the coagulation process. After production, the fibres were stored in a desiccator.

To ensure clear identification, the powder and granular PHAs will be referred to as unprocessed PHAs from now on. Fibres produced from 100% of each PHA will be labelled as neat fibres. When necessary, the fibres will be specifically identified by the PHA from which they originated.

2.4. Morphological Analyses

Morphological analysis of the produced fibres was performed using a scanning electron microscope (Zeiss EVO 10, Zeiss, Jena, Germany) operated at an accelerating voltage of 20 kV. Prior to imaging, the fibres were coated with a thin layer of gold (Au) using a BIO-RAD SC502 sputter-coater. The average of the fibres' diameters was determined by conducting 100 measurements on three micrographs. Images at a magnitude of 500 \times were used and processed using ImageJ[®] software (version 1.44, National Institutes of Health, Bethesda, MD, USA).

2.5. Chemical Analysis

A Spectrum One Perkin Elmer spectrophotometer with a diamond crystal was used. Each spectrum was obtained in the transmittance mode by accumulating 45 scans with a resolution of 4 cm⁻¹ in the range of 400 to 4000 cm⁻¹. Spectra were collected in triplicate.

To assess the degree of crystallinity and chain alignment, the absorbance ratio I_{1722}/I_{1378} was calculated. The absorption band at 1722 cm⁻¹ corresponds to the C=O stretching vibration of the carbonyl group, commonly associated with crystalline domains. The 1378 cm⁻¹ band is assigned to the symmetric bending vibrations of methyl (CH₃) groups, which are more prominent in amorphous regions. The ratio of these two absorbances provides a relative measure of the material's crystalline-to-amorphous content.

2.6. Thermal Analysis

Thermal degradation behaviour was assessed by weight loss monitoring with a temperature increase in the range of 30–700 °C at a heating rate of 20 °C/min under a synthetic air atmosphere and flow rate of 40 mL/min on a TGA 209 F1 Libra by Netzsch (Selb, Germany), using alumina pans. The results were plotted as the percentage of weight loss vs. temperature. Differential thermogravimetric (DTG) analysis was additionally conducted to identify the ranges of temperature at which the most significant degradation peaks were registered.

The thermal properties of unprocessed PHAs and fibres were evaluated using a Mettler Toledo DSC 3+ differential scanning calorimeter equipped with STARe software (version V17.00). Samples were submitted to two heating cycles: the first heating step from −40 to 200 °C at 5 °C/min, followed by holding at 200 °C for 3 min before cooling to −40 °C at 5 °C/min. Samples were reheated to 200 °C at the same heating rate. All tests were conducted in triplicate under a dynamic nitrogen atmosphere.

2.7. Mechanical Analyses

The fibres were tested for their linear mass, tensile strength, elongation, and tenacity by the vibroscope method according to EN ISO 1973:2021 [40] + EN ISO 5079:2020 [41] and their lengths were determined according to NP 1874:1982 [42] using a Favigraph from Textechno Herbert Stein GmbH & Co. KG (Monchengladbach, Germany). The tests were conducted at a clamping length of 10 mm and 5 mm/min test speed. The pre-load

weight needed to stretch the fibres according to the linear density was 100 mg. Twenty-five measurements were conducted for each sample.

3. Results and Discussion

3.1. Optimisation of the PHA Fibre Production Process

In the wet-spinning technique, factors such as the type of solvent used, the type and conditions of the coagulation bath, the concentration of the solution, and the spinning rate all play a major role in determining the morphology, molecular alignment, and mechanical properties of the resulting fibres [43,44].

Among the solvents tested, chloroform was the most suitable for fully dissolving the PHAs at all concentrations tested in a faster rate of dissolution. Chloroform was also the only solvent that enabled fibre production from ethanolic coagulation baths. Among the coagulation baths tested, ethanol demonstrated superior performance, enabling more efficient fibre coagulation compared with other non-solvents. Following systematic optimisation, a polymer concentration of 15% (*w/v*) was selected, as it supported the successful production of wet-spun fibres without clogging and allowed for continuous collection from the coagulation bath. Concentrations of 10% and 20% (*w/v*) were excluded from further analysis, as they did not consistently support effective fibre formation across all polymer types. Specifically, 20% (*w/v*) PHA solutions often led to needle clogging, impeding the wet-spinning process, while fibres produced from 10% (*w/v*) solutions were too fragile and frequently broke during removal from the coagulation bath. Based on production feasibility and post-collection fibre integrity, only the 15% (*w/v*) concentration was deemed suitable for fibre fabrication. Accordingly, all results presented in this study refer exclusively to fibres produced at this concentration.

A proper coagulation rate is crucial for producing fibres with structural integrity [45]. Therefore, identifying the correct combination of processing parameters is essential for forming stretchable polymeric fibres. This study found that PHA solutions prepared in chloroform and extruded into an ethanol-based coagulation bath at a flow rate of 0.07 mL/min successfully produced wet-spun fibres from all PHAs studied and their blends.

3.2. Morphological and Diameter Analysis of the PHA-Produced Fibres

SEM micrographs and fibre diameters are presented in Figure 1. High-magnification micrographs of the produced fibres reveal distinct morphological and shape differences. A spongy morphology was observed exclusively in neat PHBHHx fibres (Figure 1A). This morphological characteristic in PHBHHx wet-spun fibres was previously reported by Puppi et al. [37] and Mota et al. [46]. This effect has been attributed to solvent/non-solvent counter-diffusion during polymer solution coagulation, leading to phase separation into polymer-rich and a polymer-poor phases [25,43,46]. The spongy effects have been identified as beneficial features, as they positively influence the biodegradation rate [37].

Neat PHA.A.2.3.1.1 (Figure 1B) and PHA.C.3.3.1.4 (Figure 1C) fibres, despite showing some surface irregularities and not being entirely smooth, did not exhibit polymer-poor phases like the spongy effect observed in neat PHBHHx fibres. Among the individual fibres, the neat PHA.C.3.3.1.4 fibres exhibited a more uniform and rounded geometry. The average fibre diameters, summarised in Figure 2, were determined by randomly measuring 50 points on each fibre. The calculated average diameters for neat PHBHHx, PHA.A.2.3.1.1, and PHA.C.3.3.1.4 fibres were $65.54 \pm 7.34 \mu\text{m}$, $164.98 \pm 18.12 \mu\text{m}$, and $84.88 \pm 11.05 \mu\text{m}$, respectively. As shown, the fibres produced from the commercial polymer PHBHHx exhibited the smallest diameters. Similar diameter values for PHBHHx fibres, ranging between 47 and 76 μm , were also reported by Puppi et al. and Mota et al. [34,43].

Among both PHA.C.3.3.1.4 and PHA.A.2.3.1.1 fibres, the former also exhibited smaller diameters (Figure 2).

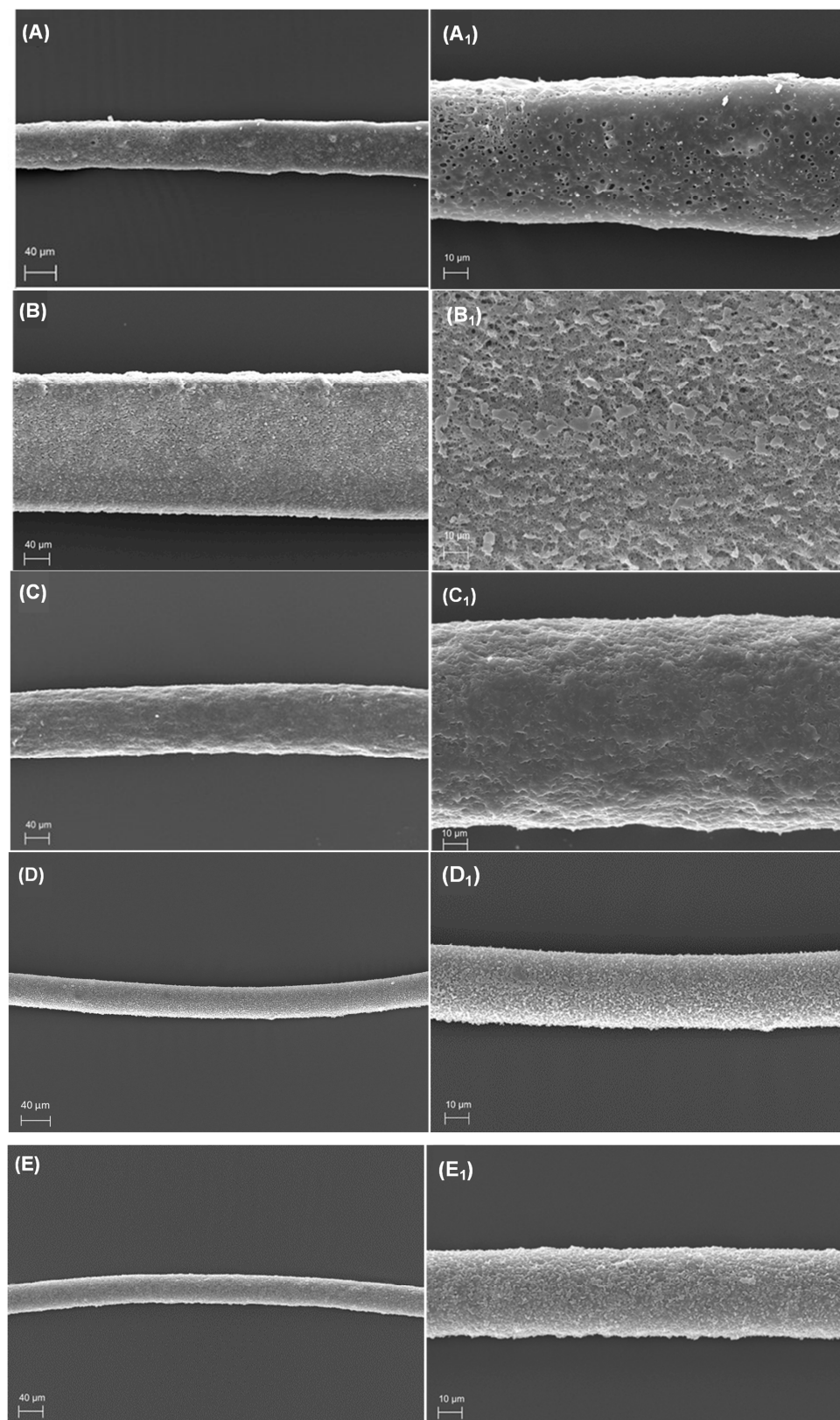


Figure 1. SEM micrographs of the wet-spun fibres produced: PHBHHx (A), PHA.A.2.3.1.1 (B), PHA.C.3.3.1.4 (C), PHA.C.3.3.1.4/PHBHHx (D), and PHA.C.3.3.1.4/PHA.A.2.3.1.1 (E). All left micrographs are shown with a magnification of 500 \times , while all right micrographs have a magnification of 1500 \times .

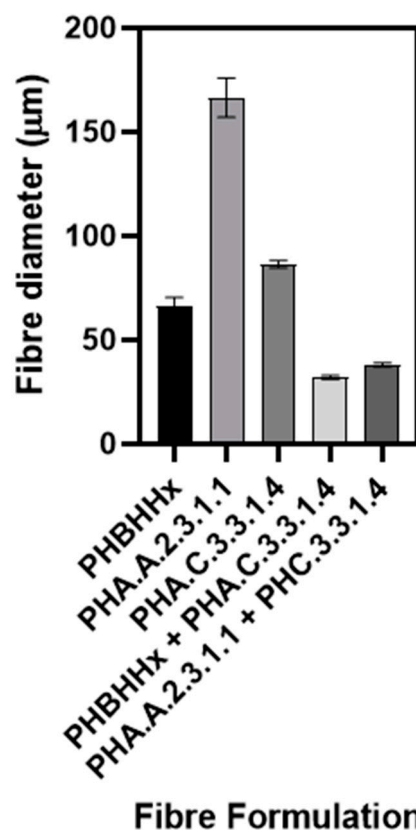


Figure 2. Diameter measurements of all fabricated fibres. The Kruskal–Wallis test was used, with multiple comparisons between different fibre formulations, to determine the statistical significance of the diameter distribution of the different PHA wet-spun fibres. A p -value < 0.001 was observed for all formulations (a comprehensive statistical analysis is provided in the Supplementary Materials).

For the blended fibres (Figure 1D,E), the combination of PHAs enhanced fibre geometry and reduced diameter, resulting in more rounded and thinner fibres, compared with the neat ones. Moreover, the blended fibres demonstrated greater uniformity in diameter, as indicated by the smaller standard deviation values from the diameter measurements, as detailed in Table S1. These benefits of blended polymeric fibres can be attributed to improved spinnability and favourable phase interactions between the PHAs, which facilitate better packing and enhance stretching and thinning during spinning. Additionally, the presence of different polymers has been reported to influence solvent evaporation and polymer coagulation processes, often leading to tighter packing and smaller diameters [47,48].

In that regard, PHA.C.3.3.1.4/PHBHHx blended fibres displayed the most uniform cylindrical shape (Figure 1D), a result further supported by the smallest standard deviation values observed among all fibres (Figure 2 and Table S1). Notably, these fibres, despite having PHBHHx in their composition, did not present a spongy structure as observed for neat PHBHHx fibres. This absence of the spongy morphology may be attributed to the higher concentration of PHA.C.3.3.1.4, which likely mitigated the phase separation typically induced during the coagulation process by the presence of PHBHHx. In terms of diameter analysis, the PHA.C.3.3.1.4/PHBHHx fibres exhibited the smallest diameters amongst all fibres produced, measuring approximately $31.46 \pm 4.22 \mu\text{m}$. PHA.C.3.3.1.4/PHA.A.2.3.1.1 blended fibres also displayed small diameters of approximately $37.48 \pm 4.66 \mu\text{m}$. These data shows that PHA.C.3.3.1.4 exhibits excellent blending and packing capabilities with the other polymers used, enhancing their spinnability and, consequently, their final morphological properties. Furthermore, the fibre diameters differed significantly across all groups, with high statistical significance (as shown in the Supplementary Materials).

3.3. Chemical Analysis

Distinct absorption peaks were observed in similar regions of the FTIR spectra of both unprocessed PHAs and their fibres (Figure 3). The prominent absorption band at 1720 cm^{-1} corresponds to the carbonyl ($\text{C}=\text{O}$) stretching of the ester group, while another band at 1276 cm^{-1} is attributed to the $-\text{CH}$ group. These bands are commonly recognised as characteristic markers for PHA. Another typical band in the FTIR spectra of PHAs is the absorption band observed around 1378 cm^{-1} , which is commonly attributed to the symmetric bending vibration of methyl (CH_3) groups [49,50]. Additionally, a series of bands between 1000 and 1300 cm^{-1} represent the stretching of the $\text{C}-\text{O}$ bond in the ester group. The bands at 2981 and 2928 cm^{-1} signify the presence of methyl (CH_3) and methylene (CH_2) asymmetric and symmetric stretching modes, respectively [51].

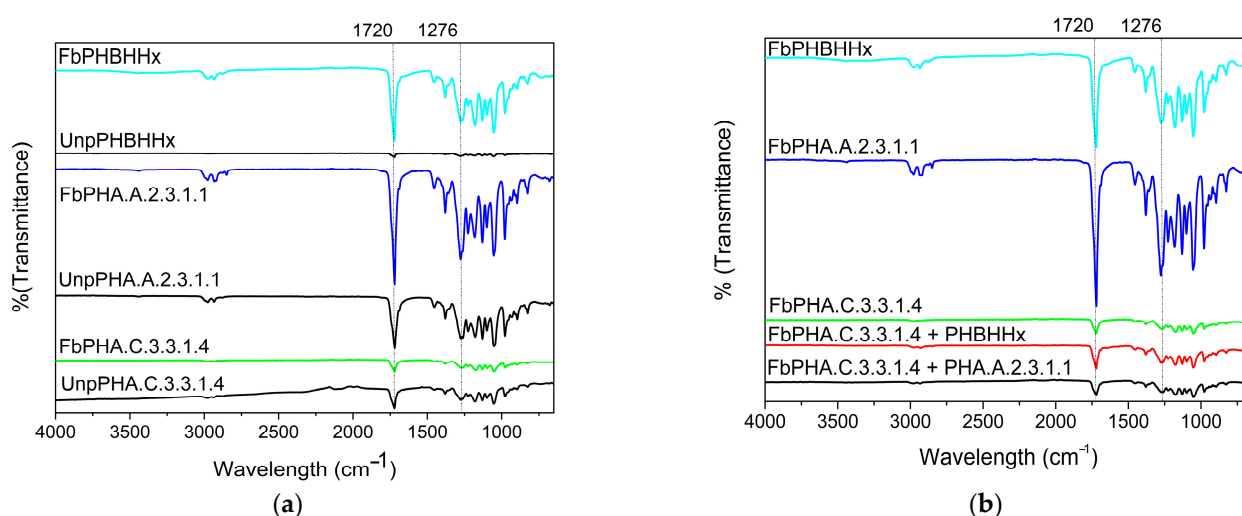


Figure 3. ATR-FTIR characterisation of the PHAs, between unprocessed and PHA fibres (a) and between only the fibres produced (b).

No differences were observed between the FTIR spectra of unprocessed PHAs and their wet-spun fibres, indicating that the polymer molecular structure was not affected by the wet-spinning process.

The I_{1722}/I_{1378} absorbance ratio—corresponding to vibrations associated with the crystalline (1722 cm^{-1}) and amorphous (1378 cm^{-1}) regions of PHAs—can be used to estimate the alignment of functional groups at the molecular scale (Table 2). The unprocessed PHBHHx polymer (commercial) exhibited the highest degree of molecular alignment, indicative of a more organised structure. Upon processing into fibres, a reduction in this ratio was observed, suggesting partial disruption of the structural order. A similar trend was noted for the chemically synthesised PHAs, which also experienced a loss of molecular alignment after fibre formation. Among these, the fibres produced from PHA.A.2.3.1.1 retained a relatively higher level of functional group alignment. In contrast, the composite fibres formed from a blend of both chemically synthesised PHAs exhibited the lowest ratio, reflecting greater structural disorganisation. Although this spectroscopic approach provides meaningful insight into the molecular arrangement, it should be complemented with additional characterisation techniques, as discussed in the following section.

Table 2. I1722/I1378 data.

		I ₁₇₂₂ /I ₁₃₇₈
Unprocessed polymers	PHBHHx	3.94
	PHA.A.2.3.1.1	2.52
	PHA.C.3.3.1.4	2.06
Fibres	PHBHHx	2.91
	PHA.A.2.3.1.1	3.79
	PHA.C.3.3.1.4	2.49
	PHBHHx/PHA.C.3.3.1.4	2.56
	PHA.C.3.3.1.4/PHA.A.2.3.1.1	2.20

3.4. Thermal Characterisation

TGA and DSC analyses were conducted to assess the thermal stability and structural characteristics of both the unprocessed polymers and their wet-spun fibres.

In this context, Figure 4a,b display the TGA and DTG thermograms, respectively, of the unprocessed polymers (UnpPHAs) and the produced fibres (FbPHAs). Table 3 presents the main degradation events of TGA, as well as glass transition temperature (T_g), melting temperature (T_m), and level crystallinity (X_c) from the second heating scans.

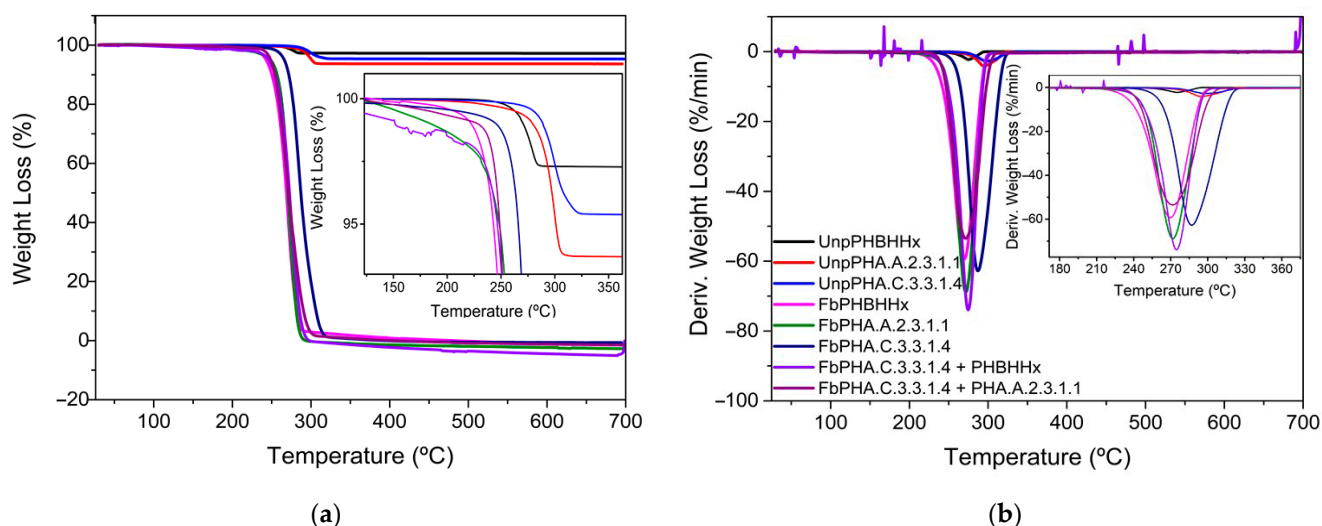


Figure 4. TGA thermograms showing weight loss (a) and derivative weight loss (b) profiles of the unprocessed PHAs (UnpPHAs) and PHA fibres (FbPHAs).

Table 3. Thermal characterisation data of unprocessed polymers and corresponding fibres determined by TGA and DSC.

		T _{onset} (°C)	T _{Max} (°C)	% Mass Loss	T _g (°C)	T _m (°C)	X _c (%)
Unprocessed polymers	PHBHHx	263.41	275.7	2.80	−3.44	103.3/119.9	24.9
	PHA.A.2.3.1.1	286.82	297.8	6.20		135.8/157.6	42.9
	PHA.C.3.3.1.4	288.21	300.4	4.60	−24.8	167.2	19.7
Fibres	PHBHHx	240.10	270.0	97.46	-	110.8/130.6	10.9
	PHA.A.2.3.1.1	252.31	272.0	100.71	-	162.6	25.1
	PHA.C.3.3.1.4	267.32	292.0	98.71	-	171.1	25.0
	PHBHHx/PHA.C.3.3.1.4	248.30	274.0	100.28	-	158.3	11.0
	PHA.C.3.3.1.4/PHA.A.2.3.1.1	243.40	272.0	98.06	-	166.6	46.4

TGA evaluations revealed that the unprocessed PHAs exhibited higher degradation temperatures and lower mass loss compared with the produced fibres (Table 3). This is likely due to their more compact molecular structure and higher crystallinity [52]. Among the unprocessed polymers evaluated, PHBHHx (the commercial polymer) exhibited the

lowest thermal stability. Its degradation step occurs the fastest, and starts from almost 260 °C, being complete at approximately 284 °C. These values are also aligned with the low T_m and X_c determined for unprocessed polymer PHBHHx, as shown in Table 3. These thermal structural features are consistent with those in some studies already carried out [51–53]. The thermal degradation behaviour of PHBHHx was characterised by the formation of shorter chain fragments with carboxylic terminal groups. Crotonic acid is produced as a by-product through a random chain scission mechanism [53]. In contrast, the partially synthesised P3HB polymers used, such as PHA.A.2.3.1.1 and PHA.C.3.3.1.4, exhibited higher thermal resistance. These unprocessed polymers displayed the highest onset and maximum degradation temperatures, as easily seen in Figure 4. These features may be attributed to the renowned high crystallinity of PH3B [54,55]. Among the unprocessed polymers, PHA.A.2.3.1.1 exhibited the highest degree of crystallinity (X_c) and a high I_{1722}/I_{1378} ratio, indicative of the presence of large, well-formed crystals and a pronounced molecular chain alignment. In contrast, PHA.C.3.3.1.4 showed the lowest glass transition temperature (T_g) and crystallinity (X_c), suggesting that it contains more flexible chains or smaller side groups [56]. However, its relatively high melting temperature (T_m) implies stronger intermolecular interactions, which is consistent with the exceptional elongation capacity observed in mechanical testing [57]. These DSC findings are corroborated by the FTIR data, as reflected in the corresponding I_{1722}/I_{1378} ratios.

In the case of the unprocessed PHBHHx polymer, although it showed a crystallinity of 24.9% as measured by DSC, it exhibited the highest I_{1722}/I_{1378} ratio (3.94). This suggests that, while the material may not contain a high proportion of large crystalline domains, its polymer chains are highly aligned at the molecular level.

Regarding the fibres produced, their thermal stability is lower compared with that of the unprocessed polymers which may occur due to increased amorphousness, processing-induced defects, and the presence of solvents [58,59]. These effects may have also arisen due to the low feed rate used during extrusion. This may have contributed to the incomplete polymer chain alignment and molecular orientation, resulting in a higher mass loss during degradation, ranging from 97% to 100%. According to the literature, a faster coagulation rate promotes the rapid formation of a solidified outer ‘skin’, followed by gradual solidification of the fibre core. This mechanism facilitates the development of an oriented fibrous structure, which enhances molecular packing and increases fibre crystallinity. As a result, the thermal stability of the fibres is significantly improved [27,60]. For this reason, wet-spun fibres generally exhibit higher crystallinity than their corresponding polymer granules, primarily due to the molecular alignment induced during the spinning process [61,62]. However, in our study, with the exception of the PHA.C.3.3.1.4 fiber, all wet-spun fibers exhibited lower crystallinity than their corresponding unprocessed polymers, as evidenced by the DSC results (Table 3). This reduction in crystallinity may be attributed to the low feed rates applied during spinning, which likely limited the maturation of crystals, as previously discussed. However, the fibers of PHA.C.3.3.1.4 and PHA.A.2.3.1.1, compared with their granule forms, appeared to exhibit enhanced structural organisation, as evidenced by the increase in their I_{1722}/I_{1378} ratios following fiber processing (Table 1). Regarding the T_m values, the highest values were observed on fibres, suggesting that the bonds established during extrusion were stronger than those on unprocessed PHAs.

Notably, the blended fibres demonstrated excellent miscibility between the constituent polymers, as evidenced by the presence of a single maximum degradation temperature (clearly visible in the DTG curves) and a single melting temperature (T_m). However, distinct spikes were observed in the DTG thermograms of the blended fibres composed of PHA.C.3.3.1.4 and PHBHHx. These anomalies may be attributed to instrumental effects, surface-related phenomena, or sample preparation issues.

Among the blends, fibres composed of PHA.C.3.3.1.4/PHA.A.2.3.1.1 exhibited the highest crystallinity values. This, together with their elevated T_m values, highlights the remarkable ability of these polymers to achieve effective chain blending. These findings are further supported by the observation of the smallest fibre diameters and most uniform (rounded) morphologies in this blend. However, its I_{1722}/I_{1378} ratio is lower compared with that of the blended fibres, suggesting that, while well-organised crystals may be present, the overall molecular alignment could have been disrupted during the wet-spinning process.

3.5. Mechanical Properties of the PHAs-Produced Fibres

The mechanical testing results presented in Table 4 were analysed in terms of linear mass, tenacity, and elongation at break for all five types of fibres. Notably, the neat PHA.A.2.3.1.1 and PHC.3.1.1.4 fibres exhibited the highest linear mass. Although all fibres were produced under identical technical conditions, these polymers demonstrated higher swelling of their extruded polymeric chains as they exited the needle. These values surpass those reported by Singhi et al. in their development of wet-spun PH4B fibres [28].

Table 4. Linear mass, tenacity and elongation of fibres produced, evaluated at a displacement rate of 5 mm/min. Data are expressed as the mean \pm C.V. (%) ($n = 25$).

Properties	PHBHHx	PHA.A.2.3.1.1	PHA.C.3.3.1.4	PHA.C.3.3.1.4/PHBHHx	PHA.C.3.3.1.4/PHA.A.2.3.1.1
Linear Mass (dtex)	1.65 \pm 44.9	3.96 \pm 64.0	4.12 \pm 57.9	1.46 \pm 37.7	0.96 \pm 11.40
Tenacity (cN/dtex)	0.4	0.4	0.4	0.2	0.4
Elongation (%)	18 \pm 180.4	0.9 \pm 43.7	136 \pm 90.5	74 \pm 98.1	10 \pm 144.7

In contrast, the blended fibres exhibited a lower linear mass compared with that of the neat fibres. This observation aligns with the findings from morphological and diameter analyses, which revealed that the blended fibres were thinner and more uniformly rounded.

The tenacity values of all the fibres were similar and notably low. This could be attributed to the low feed rates used during the extrusion process. Insufficient feed rates can disrupt the consistency of polymer flow, leading to incomplete coagulation and poor alignment of polymer chains. This effect is also reflected in the reduced crystallinity values observed in previous studies [34,63]. These factors led to fibres with reduced tenacity.

Among all the fibres tested, the neat PHA.C.3.3.1.4 demonstrated the highest elongation at break, reaching around 136%. This exceptional elongation can be attributed to increased polymer chain entanglements [64]. Additionally, this high elongation value aligns with the high T_m values and low crystallinity observed in its DSC curves, as shown in Table 3. It is well-documented in the literature that polymers with lower crystallinity typically exhibit higher elongation at break [65]. This condition is also supported by the mechanical values obtained for the PHA.A.2.3.1.1 fibres. As shown in Table 3, the PHA.A.2.3.1.1 fibre exhibited the highest crystallinity, which corresponded to the lowest elongation values.

For the blended fibres, the incorporation of PHA.C.3.3.1.4 into PHBHHx and PHA.A.2.3.1.1 significantly enhanced their elongation properties owing to the superior elongation capability of PHA.C.3.3.1.4. Specifically, elongation increased from 18 \pm 180.4% (for neat PHBHHx fibres) and 0.9 \pm 43.7% (for neat PHA.A.2.3.1.1 fibres) to 74 \pm 98.1% and 10 \pm 144.7%, respectively, in blends containing PHA.C.3.3.1.4. These values are consistent with those obtained in previous analyses, further supporting the idea that blending enhances properties by promoting strong bond formation between the polymers.

Although the coefficients of variation observed are relatively high (Table 4), they are consistent with values reported in the literature for fibre mechanical testing, where variability is common due to structural and dimensional heterogeneity.

4. Conclusions

Wet-spun fibres were successfully produced from different PHAs at a 15% concentration, demonstrating distinct morphological, thermal, and mechanical properties. Morphological analysis revealed that neat PHBHHx fibres exhibited a spongy structure due to phase separation during coagulation, a feature absent in neat PHA.C.3.3.1.4 fibres, which displayed a more uniform and rounded geometry. Blended fibres achieved smaller and more uniform diameters, with the PHA.C.3.3.1.4/PHBHHx blend showing the smallest and most consistent morphology. FTIR analyses showed characteristic bands in both PHA unprocessed and fibres FTIR spectra. No differences were observed between those different structures, indicating that wet-spinning processing does not affect the molecular structure of each polymer. FTIR analysis also provided insights into the enhancement of structural alignment induced by the wet-spinning process, particularly in the case of individually synthesised PHAs.

Thermal analysis indicated that unprocessed PHA polymers were more thermally stable than the wet-spun fibres, with PHBHHx identified as the most thermally vulnerable. Blended fibres, however, exhibited enhanced miscibility and efficient chain alignment, reflected in higher crystallinity and melting temperatures compared with neat fibres. Mechanical testing further highlighted the superior elongation at break of neat PHA.C.3.3.1.4 fibres, likely due to improved polymer chain entanglements and stronger inter-polymer bonding. The findings also highlight the critical role of feed rate during wet spinning, as lower feed rates were associated with increased fibre amorphousness and processing-induced defects. These structural limitations adversely impact both the thermal stability and mechanical strength of the fibres. Consequently, future research should aim to optimise feed rate and other key processing parameters to improve fibre quality and production efficiency. The potential implementation of post-drawing or annealing techniques also warrants further investigation, as these processes may significantly enhance molecular alignment and, consequently, increase the crystallinity of the fibres—leading to improved overall material performance. This step would likely be necessary to achieve tenacity values comparable to those of commercially available polyester fibres, which typically range from 2.6 to 5.7 cN/dtex. In the present study, however, no post-drawing or annealing processes were applied, as the primary objective was to evaluate the influence of individual polymers on the structural and physicochemical properties of the resulting fibres. Furthermore, this work demonstrates—for the first time—the feasibility of blending partially synthesised PHAs as a viable strategy to tailor fibre properties through inter-polymer interactions, opening new avenues for expanding the application potential of PHA-based fibres across various fields.

Supplementary Materials: The following supporting information can be downloaded at: <https://www.mdpi.com/article/10.3390/fib13080111/s1>, Figure S1. Distribution of individual diameters of wet-spun fibres; Figure S2. Distribution of diameters of individual fibres; Table S1. Descriptive analyses of each individual PHA fibre produced; Table S2. Kruskal–Wallis test results for fiber diameter measurements among groups. Table S3. Statistical significance of the diameter distribution among various PHA wet-spun fibre formulations.

Author Contributions: Conceptualisation, M.A.T. and C.G.; methodology, M.A.T. and C.G.; validation, H.V., C.G. and C.S.; formal analysis, C.S.; investigation, M.A.T., I.L. and R.G.; writing—original draft preparation, M.A.T.; writing—review and editing, H.V. and C.G.; supervision, H.V., C.G. and C.S.; project administration, H.V. All authors have read and agreed to the published version of the manuscript.

Funding: This work was carried out under the Waste2BioComp project—Converting organic waste into sustainable bio-based components, GA 101058654, funded under the topic HORIZON-CL4-2021-TWIN-TRANSITION-01-05 of the Horizon Europe 2021–2027 programme.

Data Availability Statement: The original contributions presented in this study are included in the article/Supplementary Materials. Further inquiries can be directed at the corresponding authors.

Acknowledgments: The authors are also greatly grateful to Waste2BioComp project funded under the topic HORIZON-CL4-2021-TWIN-TRANSITION-01-05 of the Horizon Europe 2021–2027 programme.

Conflicts of Interest: The authors declare no conflicts of interest.

References

1. Nayanathara Thathsarani Pilapitiya, P.G.C.; Ratnayake, A.S. The World of Plastic Waste: A Review. *Clean. Mater.* **2024**, *11*, 100220. [CrossRef]
2. Atiweish, G.; Mikhael, A.; Parrish, C.C.; Banoub, J.; Le, T.A.T. Environmental Impact of Bioplastic Use: A Review. *Heliyon* **2021**, *7*, e07918. [CrossRef] [PubMed]
3. Kumar, R.; Lalnundiki, V.; Shelare, S.D.; Abhishek, G.J.; Sharma, S.; Sharma, D.; Kumar, A.; Abbas, M. An Investigation of the Environmental Implications of Bioplastics: Recent Advancements on the Development of Environmentally Friendly Bioplastics Solutions. *Environ. Res.* **2024**, *244*, 117707. [CrossRef]
4. ResearchAndMarkets.com. *Bioplastics Market Size, Share & Trends Analysis Report by Product (Biodegradable, Non-Biodegradable), Application (Packaging, Agriculture, Automotive & Transportation, Electronics, Textile), Region, and Segment Forecasts*; Dublin, Ireland, 2023. Available online: <https://www.researchandmarkets.com/reports/6024551/bioplastics-market-size-share-and-trends-analysis?srsid=AfmBOoqtDPyzilPlygEmQ1CfTTXgDFKqnk9XB6KHY8JHZYXDqAbZbeO2> (accessed on 11 August 2025).
5. Rosenboom, J.G.; Langer, R.; Traverso, G. Bioplastics for a Circular Economy. *Nat. Rev. Mater.* **2022**, *7*, 117–137. [CrossRef]
6. Zhao, X.; Wang, Y.; Chen, X.; Yu, X.; Li, W.; Zhang, S.; Meng, X.; Zhao, Z.-M.; Dong, T.; Anderson, A.; et al. Sustainable Bioplastics Derived from Renewable Natural Resources for Food Packaging. *Matter* **2023**, *6*, 97–127. [CrossRef]
7. Vanheusden, C.; Vanminsel, J.; Reddy, N.; Ethirajan, A.; Buntinx, M. Fabrication of Poly(3-Hydroxybutyrate-Co-3-Hydroxyhexanoate) Fibers Using Centrifugal Fiber Spinning: Structure, Properties and Application Potential. *Polymers* **2023**, *15*, 1181. [CrossRef]
8. Valentina, S.; Blanco, I. Polymers Analogous to Petroleum-Derived Ones for Packaging and Engineering Applications. *Polymers* **2020**, *12*, 1641. [CrossRef]
9. Ali, S.S.; Abdelkarim, E.A.; Elsamahy, T.; Al-Tohamy, R.; Li, F.; Kornaros, M.; Zuurro, A.; Zhu, D.; Sun, J. Bioplastic Production in Terms of Life Cycle Assessment: A State-of-the-Art Review. *Environ. Sci. Ecotechnology* **2023**, *15*, 100254. [CrossRef]
10. Behera, S.; Priyadarshane, M.; Vandana; Das, S. Polyhydroxyalkanoates, the Bioplastics of Microbial Origin: Properties, Biochemical Synthesis, and Their Applications. *Chemosphere* **2022**, *294*, 133723. [CrossRef]
11. Mai, J.; Kockler, K.; Parisi, E.; Chan, C.M.; Pratt, S.; Laycock, B. Synthesis and Physical Properties of Polyhydroxyalkanoate (PHA)-Based Block Copolymers: A Review. *Int. J. Biol. Macromol.* **2024**, *263*, 130204. [CrossRef] [PubMed]
12. Sanhueza, C.; Acevedo, F.; Rocha, S.; Villegas, P.; Seeger, M.; Navia, R. Polyhydroxyalkanoates as Biomaterial for Electrospun Scaffolds. *Int. J. Biol. Macromol.* **2019**, *124*, 102–110. [CrossRef]
13. Naser, A.Z.; Deiab, I.; Darras, B.M. Poly(Lactic Acid) (PLA) and Polyhydroxyalkanoates (PHAs), Green Alternatives to Petroleum-Based Plastics: A Review. *RSC Adv.* **2021**, *11*, 17151–17196. [CrossRef] [PubMed]
14. Madison, L.L.; Huisman, G.W. Metabolic Engineering of Poly(3-Hydroxyalkanoates): From DNA to Plastic. *Microbiol. Mol. Biol. Rev.* **1999**, *63*, 21–53. [CrossRef]
15. Hu, D.; Chung, A.-L.; Wu, L.-P.; Zhang, X.; Wu, Q.; Chen, J.-C.; Chen, G.-Q. Biosynthesis and Characterization of Polyhydroxyalkanoate Block Copolymer P3HB- b -P4HB. *Biomacromolecules* **2011**, *12*, 3166–3173. [CrossRef]
16. Garcia-Garcia, D.; Fenollar, O.; Fombuena, V.; Lopez-Martinez, J.; Balart, R. Improvement of Mechanical Ductile Properties of Poly(3-Hydroxybutyrate) by Using Vegetable Oil Derivatives. *Macromol. Mater. Eng.* **2017**, *302*, 1600330. [CrossRef]
17. Tan, D.; Wang, Y.; Tong, Y.; Chen, G.-Q. Grand Challenges for Industrializing Polyhydroxyalkanoates (PHAs). *Trends Biotechnol.* **2021**, *39*, 953–963. [CrossRef] [PubMed]
18. McAdam, B.; Brennan Fournet, M.; McDonald, P.; Mojicevic, M. Production of Polyhydroxybutyrate (PHB) and Factors Impacting Its Chemical and Mechanical Characteristics. *Polymers* **2020**, *12*, 2908. [CrossRef] [PubMed]
19. Alm Mustafa, W.; Grishchuk, S.; Sebastian, J.; Schubert, D.W.; Grun, G. Improving I-P3HB Window: Solution-Casting with a-P3HB and P34HB. *J. Appl. Polym. Sci.* **2025**, *142*. [CrossRef]
20. Luo, Z.; Wu, Y.; Li, Z.; Loh, X.J. Recent Progress in Polyhydroxyalkanoates-Based Copolymers for Biomedical Applications. *Biotechnol. J.* **2019**, *14*, 1900283. [CrossRef]

21. Almustafa, W.; Schubert, D.W.; Grishchuk, S.; Sebastian, J.; Grun, G. Chemical Synthesis of Atactic Poly-3-Hydroxybutyrate (a-P3HB) by Self-Polycondensation: Catalyst Screening and Characterization. *Polymers* **2024**, *16*, 1655. [\[CrossRef\]](#)
22. Odian, G. *Principles of Polymerization*, 4th ed.; John Wiley & Sons: Hoboken, NJ, USA, 2004.
23. Uddin, M.K.; Novembre, L.; Greco, A.; Sannino, A. Polyhydroxyalkanoates, A Prospective Solution in the Textile Industry—A Review. *Polym. Degrad. Stab.* **2024**, *219*, 110619. [\[CrossRef\]](#)
24. Miranda, C.S.; Marinho, E.; Seabra, C.L.; Evenou, C.; Lamartine, J.; Fromy, B.; Costa, S.P.G.; Homem, N.C.; Felgueiras, H.P. Antimicrobial, Antioxidant and Cytocompatible Coaxial Wet-Spun Fibers Made of Polycaprolactone and Cellulose Acetate Loaded with Essential Oils for Wound Care. *Int. J. Biol. Macromol.* **2024**, *277*, 134565. [\[CrossRef\]](#)
25. Miranda, C.S.; Silva, A.F.G.; Pereira-Lima, S.M.M.A.; Costa, S.P.G.; Homem, N.C.; Felgueiras, H.P. Tunable Spun Fiber Constructs in Biomedicine: Influence of Processing Parameters in the Fibers' Architecture. *Pharmaceutics* **2022**, *14*, 164. [\[CrossRef\]](#)
26. Kopf, S.; Åkesson, D.; Skrifvars, M. Textile Fiber Production of Biopolymers—A Review of Spinning Techniques for Polyhydroxyalkanoates in Biomedical Applications. *Polym. Rev.* **2023**, *63*, 200–245. [\[CrossRef\]](#)
27. Kundrat, V.; Matouskova, P.; Marova, I. Facile Preparation of Porous Microfiber from Poly-3-(R)-Hydroxybutyrate and Its Application. *Materials* **2019**, *13*, 86. [\[CrossRef\]](#) [\[PubMed\]](#)
28. Singhi, B.; Ford, E.N.; King, M.W. The Effect of Wet Spinning Conditions on the Structure and Properties of Poly-4-hydroxybutyrate Fibers. *J. Biomed. Mater. Res. B Appl. Biomater.* **2021**, *109*, 982–989. [\[CrossRef\]](#) [\[PubMed\]](#)
29. Degeratu, C.N.; Mabilieu, G.; Aguado, E.; Mallet, R.; Chappard, D.; Cincu, C.; Stancu, I.C. Polyhydroxyalkanoate (PHBV) Fibers Obtained by a Wet Spinning Method: Good in Vitro Cytocompatibility but Absence of in Vivo Biocompatibility When Used as a Bone Graft. *Morphologie* **2019**, *103*, 94–102. [\[CrossRef\]](#) [\[PubMed\]](#)
30. Alagöz, A.S.; Rodriguez-Cabello, J.C.; Hasirci, V. PHBV Wet-Spun Scaffold Coated with ELR-REDV Improves Vascularization for Bone Tissue Engineering. *Biomed. Mater.* **2018**, *13*, 055010. [\[CrossRef\]](#)
31. Kusmono, K.; Wildan, M.W.; Lubis, F.I. Fabrication and Characterization of Chitosan/Cellulose Nanocrystal/Glycerol Bio-Composite Films. *Polymers* **2021**, *13*, 1096. [\[CrossRef\]](#)
32. Gao, C.; He, S.; Qiu, L.; Wang, M.; Gao, J.; Gao, Q. Continuous Dry–Wet Spinning of White, Stretchable, and Conductive Fibers of Poly(3-Hydroxybutyrate-Co-4-Hydroxybutyrate) and ATO@TiO₂ Nanoparticles for Wearable e-Textiles. *J. Mater. Chem. C Mater.* **2020**, *8*, 8362–8367. [\[CrossRef\]](#)
33. Alagöz, A.S. Bone Tissue Engineering Using Macroporous Pha-Pla And Phbv Scaffolds Produced By Additive Manufacturing and Wet Spinning. Master's Thesis, Middle East Technical University, Ankara, Turkey, 2016.
34. Pecorini, G.; Braccini, S.; Simoni, S.; Corti, A.; Parrini, G.; Puppi, D. Additive Manufacturing of Wet-Spun Poly(3-hydroxybutyrate-Co-3-hydroxyvalerate)-Based Scaffolds Loaded with Hydroxyapatite. *Macromol. Biosci.* **2024**, *24*, e2300538. [\[CrossRef\]](#) [\[PubMed\]](#)
35. Kong, L.; Ziegler, G.R. Fabrication of κ -Carrageenan Fibers by Wet Spinning: Spinning Parameters. *Materials* **2011**, *4*, 1805–1817. [\[CrossRef\]](#)
36. Miranda, C.S.; Silva, A.F.G.; Seabra, C.L.; Reis, S.; Silva, M.M.P.; Pereira-Lima, S.M.M.A.; Costa, S.P.G.; Homem, N.C.; Felgueiras, H.P. Sodium Alginate/Polycaprolactone Co-Axial Wet-Spun Microfibers Modified with N-Carboxymethyl Chitosan and the Peptide AAPV for Staphylococcus Aureus and Human Neutrophil Elastase Inhibition in Potential Chronic Wound Scenarios. *Biomater. Adv.* **2023**, *151*, 213488. [\[CrossRef\]](#)
37. Puppi, D.; Chiellini, F. Wet-Spinning of Biomedical Polymers: From Single-Fibre Production to Additive Manufacturing of Three-Dimensional Scaffolds. *Polym. Int.* **2017**, *66*, 1690–1696. [\[CrossRef\]](#)
38. Abdulrahman, A.; van Walsum, G.P.; Um, B.-H. Acetic Acid Removal from Pre-Pulping Wood Extract with Recovery and Recycling of Extraction Solvents. *Appl. Biochem. Biotechnol.* **2019**, *187*, 378–395. [\[CrossRef\]](#)
39. Watkins, P. Comparing the Use of Chloroform to Petroleum Ether for Soxhlet Extraction of Fat in Meat. *Anim. Prod. Sci.* **2023**, *63*, 1445–1449. [\[CrossRef\]](#)
40. EN ISO 1973:2021; Textile Fibres—Determination of Linear Density—Gravimetric Method and Vibroscope Method. ISO: Geneva, Switzerland, 2021.
41. EN ISO 5079:2020; Textile Fibres—Determination of Breaking Force and Elongation at Break of Individual Fibres. ISO: Geneva, Switzerland, 2020.
42. NP-1874; Têxteis Fibras—Determinação Do Comprimento Por Medição Fibra e Fibra. DGQ: Lisboa, Portugal, 1982.
43. Puppi, D.; Piroso, A.; Morelli, A.; Chiellini, F. Design, Fabrication and Characterization of Tailored Poly[(R)-3-Hydroxybutyrate-Co-(R)-3-Hydroxyexanoate] Scaffolds by Computer-Aided Wet-Spinning. *Rapid Prototyp. J.* **2018**, *24*, 1–8. [\[CrossRef\]](#)
44. Yan, J.; Zhou, G.; Knight, D.P.; Shao, Z.; Chen, X. Wet-Spinning of Regenerated Silk Fiber from Aqueous Silk Fibroin Solution: Discussion of Spinning Parameters. *Biomacromolecules* **2010**, *11*, 1–5. [\[CrossRef\]](#) [\[PubMed\]](#)
45. Han, W.; Wang, L.; Li, Q.; Ma, B.; He, C.; Guo, X.; Nie, J.; Ma, G. A Review: Current Status and Emerging Developments on Natural Polymer-Based Electrospun Fibers. *Macromol. Rapid Commun.* **2022**, *43*, 2200456. [\[CrossRef\]](#) [\[PubMed\]](#)

46. Mota, C.; Wang, S.-Y.; Puppi, D.; Gazzarri, M.; Migone, C.; Chiellini, F.; Chen, G.-Q.; Chiellini, E. Additive Manufacturing of Poly[(R)-3-Hydroxybutyrate- Co -(R)-3-Hydroxyhexanoate] Scaffolds for Engineered Bone Development. *J. Tissue Eng. Regen. Med.* **2017**, *11*, 175–186. [[CrossRef](#)] [[PubMed](#)]
47. Chen, L.; Pan, D.; He, H. Morphology Development of Polymer Blend Fibers along Spinning Line. *Fibers* **2019**, *7*, 35. [[CrossRef](#)]
48. Zakaria, M.; Shibahara, K.; Nakane, K. Melt-Electrospun Polyethylene Nanofiber Obtained from Polyethylene/Polyvinyl Butyral Blend Film. *Polymers* **2020**, *12*, 457. [[CrossRef](#)]
49. Lu, H.; Kazarian, S.G.; Sato, H. Simultaneous Visualization of Phase Separation and Crystallization in PHB/PLLA Blends with In Situ ATR-FTIR Spectroscopic Imaging. *Macromolecules* **2020**, *53*, 9074–9085. [[CrossRef](#)]
50. Trakunjae, C.; Boondaeng, A.; Apiwatanapiwat, W.; Kosugi, A.; Arai, T.; Sudesh, K.; Vaithanomsat, P. Enhanced Polyhydroxybutyrate (PHB) Production by Newly Isolated Rare Actinomycetes Rhodococcus Sp. Strain BSRT1-1 Using Response Surface Methodology. *Sci. Rep.* **2021**, *11*, 1896. [[CrossRef](#)] [[PubMed](#)]
51. Ramezani, M.; Amoozegar, M.A.; Ventosa, A. Screening and Comparative Assay of Poly-Hydroxyalkanoates Produced by Bacteria Isolated from the Gavkhooni Wetland in Iran and Evaluation of Poly- β -Hydroxybutyrate Production by Halotolerant Bacterium Oceanimonas Sp. GK1. *Ann. Microbiol.* **2015**, *65*, 517–526. [[CrossRef](#)]
52. Otaru, A.J.; Alhulaybi, Z.A.; Dubdub, I. Machine Learning Backpropagation Prediction and Analysis of the Thermal Degradation of Poly (Vinyl Alcohol). *Polymers* **2024**, *16*, 437. [[CrossRef](#)]
53. Díez-Pascual, A.; Díez-Vicente, A. Poly(3-Hydroxybutyrate)/ZnO Bionanocomposites with Improved Mechanical, Barrier and Antibacterial Properties. *Int. J. Mol. Sci.* **2014**, *15*, 10950–10973. [[CrossRef](#)]
54. Di Lorenzo, M.L.; Androsch, R. Crystallization of Poly[(R)-3-Hydroxybutyrate]. In *Thermal Properties of Bio-Based Polymers*; Springer: Berlin/Heidelberg, Germany, 2019; pp. 119–142.
55. Vahabi, H.; Michely, L.; Moradkhani, G.; Akbari, V.; Cochez, M.; Vagner, C.; Renard, E.; Saeb, M.R.; Langlois, V. Thermal Stability and Flammability Behavior of Poly(3-Hydroxybutyrate) (PHB) Based Composites. *Materials* **2019**, *12*, 2239. [[CrossRef](#)]
56. Xie, R.; Weisen, A.R.; Lee, Y.; Aplan, M.A.; Fenton, A.M.; Masucci, A.E.; Kempe, F.; Sommer, M.; Pester, C.W.; Colby, R.H.; et al. Glass Transition Temperature from the Chemical Structure of Conjugated Polymers. *Nat. Commun.* **2020**, *11*, 893. [[CrossRef](#)]
57. Seymour, R.B.; Carraher, C.E. Mechanical Properties of Polymers. In *Structure—Property Relationships in Polymers*; Springer: Boston, MA, USA, 1984; pp. 57–72.
58. Puchalski, M.; Kwolek, S.; Szparaga, G.; Chrzanowski, M.; Krucińska, I. Investigation of the Influence of PLA Molecular Structure on the Crystalline Forms (α' and α) and Mechanical Properties of Wet Spinning Fibres. *Polymers* **2017**, *9*, 18. [[CrossRef](#)] [[PubMed](#)]
59. Asim, M.; Paridah, M.T.; Chandrasekar, M.; Shahroze, R.M.; Jawaid, M.; Nasir, M.; Siakeng, R. Thermal Stability of Natural Fibers and Their Polymer Composites. *Iran. Polym. J.* **2020**, *29*, 625–648. [[CrossRef](#)]
60. Park, S.; Park, J.K. Back to Basics: The Coagulation Pathway. *Blood Res.* **2024**, *59*, 35. [[CrossRef](#)]
61. Mirbaha, H.; Scardi, P.; D'Incau, M.; Arbab, S.; Nourpanah, P.; Pugno, N.M. Supramolecular Structure and Mechanical Properties of Wet-Spun Polyacrylonitrile/Carbon Nanotube Composite Fibers Influenced by Stretching Forces. *Front. Mater.* **2020**, *7*, 226. [[CrossRef](#)]
62. Pereira, C.; Pinto, T.V.; Santos, R.M.; Correia, N. Sustainable and Naturally Derived Wet Spun Fibers: A Systematic Literature Review. *Fibers* **2024**, *12*, 75. [[CrossRef](#)]
63. Consul, P.; Beuerlein, K.-U.; Luzha, G.; Drechsler, K. Effect of Extrusion Parameters on Short Fiber Alignment in Fused Filament Fabrication. *Polymers* **2021**, *13*, 2443. [[CrossRef](#)] [[PubMed](#)]
64. Kim, J.; Zhang, G.; Shi, M.; Suo, Z. Fracture, Fatigue, and Friction of Polymers in Which Entanglements Greatly Outnumber Cross-Links. *Science (1979)* **2021**, *374*, 212–216. [[CrossRef](#)] [[PubMed](#)]
65. Feijoo, P.; Samaniego-Aguilar, K.; Sánchez-Safont, E.; Torres-Giner, S.; Lagaron, J.M.; Gamez-Perez, J.; Cabedo, L. Development and Characterization of Fully Renewable and Biodegradable Polyhydroxyalkanoate Blends with Improved Thermoformability. *Polymers* **2022**, *14*, 2527. [[CrossRef](#)] [[PubMed](#)]

Disclaimer/Publisher's Note: The statements, opinions and data contained in all publications are solely those of the individual author(s) and contributor(s) and not of MDPI and/or the editor(s). MDPI and/or the editor(s) disclaim responsibility for any injury to people or property resulting from any ideas, methods, instructions or products referred to in the content.